

Grassland and forest understorey biomass emissions from prescribed fires in the southeastern United States – RxCADRE 2012

Tara Strand^{A,G}, Brian Gullett^B, Shawn Urbanski^C, Susan O'Neill^D, Brian Potter^D, Johanna Aurell^{E,F}, Amara Holder^B, Narasimhan Larkin^D, Mark Moore^D and Miriam Rorig^D

^AScion, Crown Forest Research Institute, Forestry Building, Forestry Road, Ilam, Christchurch 8041, New Zealand.

^BUS Environmental Protection Agency, Office of Research and Development, Research Triangle Park, 109 T. W. Alexander Drive, Durham, NC 27711, USA.

^CUSDA Forest Service, Rocky Mountain Research Station, 5775 US Highway 10 West, Missoula, MT 59808, USA.

^DUSDA Forest Service, Pacific Northwest Research Station, 400 North 34th Street, Suite 201, Seattle, WA 98103, USA.

^ENational Research Council Postdoctoral Fellow to the US Environmental Protection Agency, Office of Research and Development, National Risk Management Research Laboratory, Research Triangle Park, 109 T. W. Alexander Drive, Durham, NC 27711, USA.

^FPresent address: University of Dayton Research Institute, Energy Technology and Materials Division, 300 College Park Dayton, OH 45469, USA.

^GCorresponding author. Email: tara.strand@scionresearch.com

Abstract. Smoke measurements were made during grass and forest understorey prescribed fires as part of a comprehensive programme to understand fire and smoke behaviour. Instruments deployed on the ground, airplane and tethered aerostat platforms characterised the smoke plumes through measurements of carbon dioxide (CO₂), carbon monoxide (CO), methane (CH₄) and particulate matter (PM), and measurements of optical properties. Distinctions were observed in aerial and ground-based measurements, with aerial measurements exhibiting smaller particle size distributions and PM emission factors, likely due to particle settling. Black carbon emission factors were similar for both burns and were highest during the initial flaming phase. On average, the particles from the forest fire were less light absorbing than those from the grass fires due to the longer duration of smouldering combustion in the forest biomass. CO and CH₄ emission factors were over twice as high for the forest burn than for the grass burn, corresponding with a lower modified combustion efficiency and greater smouldering combustion. This dataset reveals the evolution of smoke emissions from two different commonly burned fuel types and demonstrates the complexity of emission factors.

Additional keywords: black carbon, combustion efficiency, emissions factor, particulate matter, smoke.

Received 14 September 2014, accepted 27 August 2015, published online 17 November 2015

Introduction

In many regions around the world, fire is an essential ecological process emitting particulate (Hodzic *et al.* 2007; Strand *et al.* 2011) and gaseous compounds (Goode *et al.* 1999; Aurell and Gullett 2013) into the atmosphere on a wide variety of spatial and temporal scales, driven by both natural forces and human management decisions. Particulate emissions strongly affect regional visibility (McMeeking *et al.* 2006), can cause a positive or negative climate forcing (Hobbs *et al.* 1997), and can cause inhalation health effects (Wegesser *et al.* 2009). The black carbon (BC) fraction of particulates has been found to accelerate Arctic and Greenland ice sheet melting (Bond *et al.* 2013).

The strong spectral variation in light absorption of the organic carbon fraction (i.e. brown carbon) within smoke from biomass burning contributes to atmospheric warming (Chung *et al.* 2012) and affects photochemistry (Li *et al.* 2011). Gas compounds emitted during biomass burning include greenhouse gases, tropospheric ozone precursors and other air quality pollutants (Andreae and Merlet 2001). Understanding the effects of these emissions on global climate and regional air quality requires quantification of biomass burning emissions.

Predicting wildland fire emissions requires prediction of fire occurrence and growth, fuel type consumed and combustion phase such as flaming or smouldering, and each such

prediction compounds uncertainty (French *et al.* 2011). Emission factors associated with a fuel type, combustion phase, or both, are used to estimate emissions when combined with mass of fuel consumed. Emission factors have varying ranges of uncertainty depending on the emitted chemical species (Urbanski *et al.* 2009; Akagi *et al.* 2010). Several studies have derived emission factors for a variety of North American fuel types – including southeastern USA fuels – using excess concentration data collected from prescribed fires, wildfire measurements and laboratory studies (Burling *et al.* 2011; Akagi *et al.* 2013; Yokelson *et al.* 2013). Collectively, these studies have provided reasonable estimates of emission factors for the primary gas species carbon dioxide, carbon monoxide and methane (CO_2 , CO , CH_4), which are emitted during biomass burning, and the fuel type with which they are associated. In contrast, for other emitted species such as particulate matter (PM), uncertainty remains large or unknown (Larkin *et al.* 2014).

To improve our capability to predict smoke emissions and to model smoke plume concentrations, it is necessary to develop a full understanding of a plume's suite of gas and particulate species and their concentrations both near the ground and aloft. Smoke concentration observations combined with measurements of fire behaviour and the fuel type consumed allow for a full time-lapse view of the shift in biomass emissions as it relates to the dynamic fire. The Prescribed Fire Combustion and Atmospheric, Dynamics Research Experiment (RxCADRE) 2012 was designed to collect data needed to advance fire behaviour models and further our understanding of smoke emissions (Ottmar *et al.* 2015). Three prescribed fires were ignited for the purpose of studying smoke emissions and concentrations. These fires consisted of two grass burns and one forest understorey fire. Measurements of CO_2 , CO , CH_4 , fine PM (particles $\leq 2.5 \mu\text{m}$ in aerodynamic diameter, $\text{PM}_{2.5}$), particle size distributions, BC and filter-based PM absorption in the ultraviolet (UVPM), indicative of brown carbon, were collected downwind from the fire, both near the ground and aloft. Emission measurements were compared between ground-based and aerial sampling, as well as among the grass and forest burns. Results from these measurements and how they compare to data collected in similar fuel types are detailed below.

Methods

Burn and site description

Smoke emissions and plume characteristics were measured during three large burns at Eglin Air Force Base in north-western Florida, USA. Two large grass fields (L1G and L2G) and the understorey of one large forested area (L2F) were lit by drip torch ignition from four-wheel drive utility task vehicles (UTVs). The goal of the ignition was to develop strips of fire far enough apart that individual head fires ran forward in the classic parabola shape.

Instruments to measure emissions were deployed at various ground level locations surrounding the burn units (Fig. 1) and in the air via aircraft and tethered aerostat (Table 1). The following sections describe the instruments deployed, sampling methods and data obtained during the three burns.

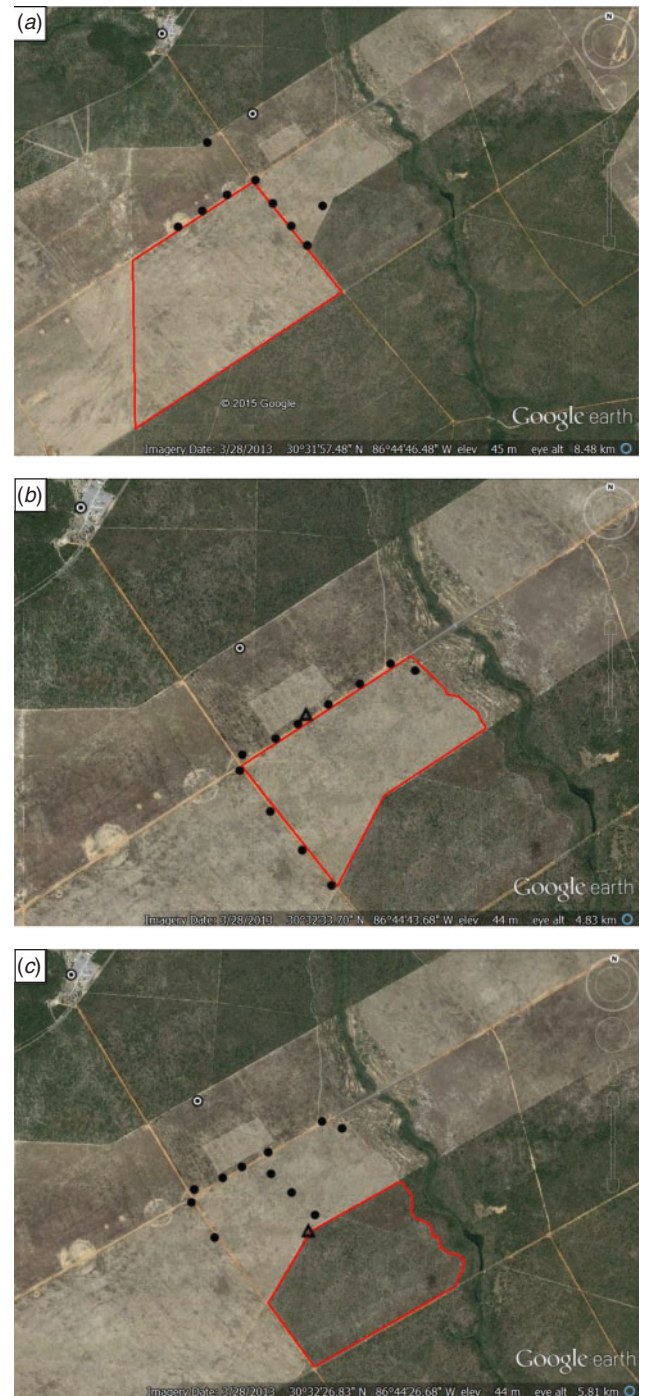


Fig. 1. Position of ground-based instruments relative to (a) L1G, (b) L2G and (c) L2F. Black dots indicate Environmental Beta Attenuation Monitors (EBAMs). Triangle shows the location of the aerostat and ground flyers as well as the ground BC instrumentation for L2G and L2F. The white and black bullseye indicates the locations of the background reference EBAMs. North is to the top of the figure.

Ground and aerostat instrumentation

Environmental Beta Attenuation Monitors (EBAMs, Met One Inc., Grants Pass, OR) arrayed around each burn measured

Table 1. Instruments deployed to measure the properties of smoke and their location relative to the burn perimeter and height above ground level (AGL)

Variables measured include carbon monoxide (CO), carbon dioxide (CO₂), methane (CH₄), particulate matter $\leq X$ μm in aerodynamic diameter (PM_X), equivalent black carbon (EBC), elemental carbon (EC), organic carbon (OC), aerosol absorption coefficient (B_{abs}), scattering coefficient (B_{scat}), size-resolved refractory black carbon (rBC) and particulate matter absorption in the ultraviolet (UVPM)

Platform	Location (m)	Height AGL (m)	Instrument	Variable
Ground	20–900 ^A	2.2	Environmental Beta Attenuation Monitors (EBAMs)	PM _{2.5}
	7 and 60 ^B	2.0	PASS-3 SP2 AE51 DustTrak 8520	B_{abs} , B_{scat} rBC EBC PM _{2.5}
Ground–flyer	7 and 60 ^B	2.0	Teflon and quartz filter samplers	PM _{2.5} (EC:OC)
			SUMMA canisters SKC Impactor sampling (via thermal–optical analysis (TOA) National Institute for Occupational Safety and Health (NIOSH) method)	CO:CO ₂ PM _{2.5} EC:OC
Aloft–flyer	7 and 60 ^B	50–110 and 45–85 ^C	DustTrak, DRX 8533 DustTrak 8520 AE51 AE52	PM ₁ , PM _{2.5} , PM ₄ and PM ₁₀ PM _{2.5} EBC, UVPM
			SUMMA canisters SKC Impactor sampling (via TOA NIOSH method) DustTrak, DRX 8533 DustTrak 8520 AE51 AE52	CO:CO ₂ PM _{2.5} EC:OC PM ₁ , PM _{2.5} , PM ₄ and PM ₁₀ PM _{2.5} EBC, UVPM
Aircraft	2000–2500 ^D	150–910	Cavity ring-down spectroscopy	CO ₂ , CO, CH ₄

^AEBAM locations relative to the burn perimeter varied depending on burn.

^BInstruments were located 7 m from L2G and 60 m from L2F burn perimeters.

^CInstruments were located 50–110 m AGL during L1F and 45–85 m AGL during L2G.

^DAircraft flew in this horizontal range for all burns.

5-min and hourly averages of PM_{2.5} concentrations. To ensure that concentrations were recorded during the burn, even under varying wind conditions, the 9 L1G and 11 L2G and L2F monitors were arrayed in two semi-circles at distances of 20 m and 850 m downwind from the burn perimeter (L1G), one semi-circle at 20 m (L2G) and a semi-circle that was roughly 900 m away from the L2F burn perimeter with a perpendicular transect running between the semi-circle and burn perimeter. Background PM_{2.5} concentrations were measured continuously throughout the RxCADRE programme at two locations: one near the burn (850 m from the perimeter) and one further away (~2.4 km) from the field site. For all monitors, air was pulled continuously through an inlet located 2.2 m above ground level (AGL). Leak tests and flow rate tests were conducted before each burn and the flow rate was calibrated if necessary.

A helium-filled tethered aerostat (4.3 m in diameter) and a ground-based UTV each carried a light-weight instrument package termed the ‘Flyer’, both were located near the fire, just outside the burn perimeter. The aerostat collected emissions at altitudes of 50–110 m AGL for the forest burn (L2F) and 45–85 m AGL for the grass burn (L2G).

The aerostat-Flyer and UTV-Flyer sampling approaches have been described in detail elsewhere (Aurell *et al.* 2011; Aurell and Gullett 2013). Flyer instruments included SUMMA canisters for CO and CO₂; batch inertial impactor sampling (SKC Inc., Eighty Four, PA) of PM_{2.5} onto a 47-mm diameter Teflon filter (2- μm pore size, constant 10 L min⁻¹); and batch impactor sampling onto quartz filters for elemental carbon and organic carbon (EC and OC) analyses via a modified, thermal–optical analysis (TOA) National Institute for Occupational Safety and Health (NIOSH) method 5040 (NIOSH 1999), as reported in Khan *et al.* (2012). Continuous and simultaneous measurements of PM₁, PM_{2.5}, PM₄ and PM₁₀ were made using a light-scattering photometer (DustTrak, DRX 8533, TSI Inc., Shoreview, MN) as well as only PM_{2.5} (DustTrak 8520, TSI Inc.). BC was measured with a single-wavelength micro-aethalometer (AE51, Aethlabs, San Francisco, CA) and a dual-wavelength aethalometer (AE52, Aethlabs) that captures the UVPM, indicative of brown carbon. Following the terminology outlined in the Petzold *et al.* (2013), BC measured by filter-based absorption in the AE51 and AE52 is referred to as equivalent black carbon (EBC), to distinguish it from other BC

measurements. Flyers were also equipped with global positioning systems (MTi-G, Xsens, Enschede, Netherlands) for position and altitude.

A second ground-based system proximally located near the burn perimeter made continuous measurements of PM optical characteristics and BC concentrations at 2 m in height during L2G and L2F burns. This system comprised a three-wavelength photoacoustic soot spectrometer (PASS-3, Droplet Measurement Technologies, Boulder, CO), a single-particle soot photometer (SP2, Droplet Measurement Technologies), a microaethalometer (AE51, Aethlabs) and a DustTrak 8520 (TSI Inc.). The PASS-3 uses a photoacoustic effect to measure the aerosol absorption coefficient (B_{abs}) and a reciprocal nephelometer to measure the scattering coefficient (B_{scat}) at 405 nm, 532 nm and 781 nm (Flowers *et al.* 2010). The SP2 measures size-resolved refractory black carbon (rBC) concentration by laser-induced incandescence (Schwarz *et al.* 2006). A capillary dilution system (DIL550, TOPAS, Dresden, Germany) was used in conjunction with the SP2 in the field to reduce rBC concentrations to within the instrument measurement range. In addition to these continuous measurements, co-located Teflon and quartz filter samples were taken for determination of PM_{2.5} mass, and EC and OC concentrations.

Aircraft instrumentation and sampling

A flight-ready cavity ring-down spectroscopy (CRDS) trace-gas analyser (Picarro Inc., Santa Clara, CA, USA, model G2401-m) was used to take continuous measurements of CO₂, CO and CH₄ with a data acquisition rate of 0.5 Hz. Urbanski (2013) provides details on the CRDS instrument and measurement technique. Two point in-flight calibrations using NIST-traceable standards were used to ensure accuracy of the CRDS measurements and quantify the measurement precision. The calibration standards were gas mixtures of CO₂, CO and CH₄ in ultrapure air (ppm \pm reported analytical uncertainty: CO₂ = 351 \pm 4 and 510 \pm 5; CO = 0.0920 \pm 0.0092 and 3.03 \pm 0.06; and CH₄ = 1.493 \pm 0.015 and 3.03 \pm 0.03) (Scott-Marrin Inc., Riverside, CA). The CRDS in-flight measurement precision was taken as the 14-s standard deviation while measuring a calibration standard. The three-fire average CRDS measurement precision was 0.251 ppm for CO₂, 0.008 ppm for CO and 0.005 ppm for CH₄. Calibrations were spaced 25–100 min apart and were applied to the raw data by linearly interpolating the calibration coefficients. The average drift in the instrument response between calibrations was 0.308 ppm for CO₂, 0.009 ppm for CO and 0.004 ppm for CH₄.

The measurement platform was a Cessna 337 aircraft. Smoke and ambient air were sampled through a 0.5-in-outside diameter (o.d.) stainless steel inlet located on the pilot window. The CRDS instrument pulled \sim 0.5 standard litres per minute off the sample line. Excess sample flow and the CRDS outflow were exhausted out the rear of the fuselage through a 0.5-in-o.d. Teflon line. The aircraft sampling equipment measured fresh smoke emissions, smoke vertical profile, plume height and smoke dispersion. Measurements of fresh emissions and smoke dispersion were obtained with horizontal flight transects in perpendicular and zigzag patterns at distances of up to 25 km downwind from the source. Measurements of the smoke

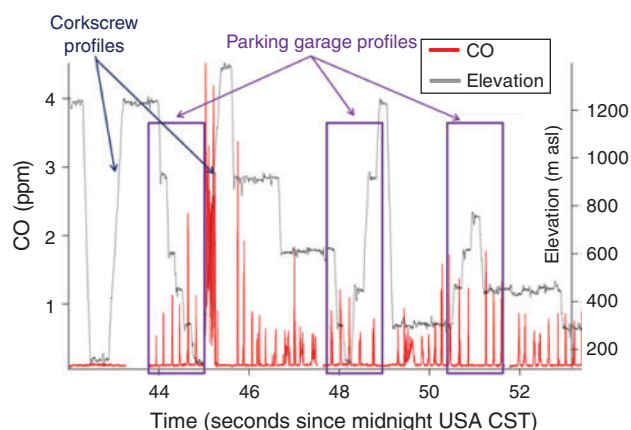


Fig. 2. Airplane vertical flight profile for the L2F fire. The grey line is the airplane altitude (m above mean sea level), and the red line is the carbon monoxide (CO) mixing ratio (ppm by volume) measured with the cavity ring-down spectroscopy trace-gas analyser. The x-axis is time in 1000 s since midnight (ssm) (e.g. 44 640 ssm is 1224 hours Central Standard Time (CST)).

concentration vertical profile (Fig. 2) and the maximum height of the smoke layer were obtained with corkscrew and parking garage flight profiles. Corkscrew profiles, centred on the plume downwind from the burn unit, were taken from above the smoke plume/layer to 150 m AGL. Parking garage vertical profiles are short (\sim 10 km) horizontal transects, roughly perpendicular to the long-axis of the smoke plume, taken at multiple altitudes ranging between 300 and 910 m AGL. The parking garage vertical profiles also provide measurements of spatial distribution of smoke emissions and dispersion. Emissions were determined from level-altitude flight segments that began in smoke-free background air, passed through the smoke plume and then re-entered the background air. A section of each flight segment before plume entry provided the background measurements used to calculate the excess mixing ratios. The background CO provided a baseline to identify the smoke plume entry and exit points and selection of the smoke sample data points.

Data analyses

Hourly and 5-min surface PM_{2.5} concentration data were similar for L1G and L2G, and L1G data are displayed. For L2F, hourly PM_{2.5} concentrations measured from all monitors were placed into a boxplot, which represented the spread of values measured during each hour of the burn.

Emission factors (EFs) for pollutants X , EF_X (in units of mass of X per mass of dry fuel consumed), were calculated for each smoke sample using the carbon mass balance method (Eqn 1) as found in Laursen *et al.* (1992) and Yokelson *et al.* (1999). The carbon (C) volatilised during combustion was calculated from mixing ratios of simultaneously sampled, background-corrected C-containing species, ΔX ($\Delta X = X_{smoke} - X_{background}$) and the C fraction (F_c) in the fuel biomass. A value of 0.5 was used for F_c based on analysis of the forest litter (Table 2) and was estimated to be the same for the grass units. Previous biomass

Table 2. Ultimate analyses of the forest litter collected before the forest understorey surface fire (L2F)

	Forest litter
Loss of mass due to water evaporation when drying (%)	17.4
Carbon (F _c) (%)	49.6
Chlorine (ppm)	849
Oxygen (%)	42.4
Hydrogen (%)	6.3
Nitrogen (%)	<0.5
Sulfur (%)	0.0585

burning emission studies have found F_c to range between 0.45 and 0.55 for the vegetation types burned in this study (Burling *et al.* 2010).

$$EF_X = F_c \times 1000 \text{ (g kg}^{-1}\text{)} \times \frac{MM_X}{12} \times \frac{\Delta X}{\Delta C_{CO_2} + \Delta C_{CO} + \Delta C_{CH_4}} \quad (1)$$

where ΔC_i are the excess mass mixing ratios of C in each emitted species X ; MM_X is the molar mass of X (g mole⁻¹) and 12 is the molar mass of C (g mole⁻¹).

For the airplane measurements, CO₂, CO and CH₄ were used in the C balance calculation as described in Urbanski 2013. Ignoring other carbon-containing species has less than a 5% effect on the EF (Urbanski 2014). The ground- and aerostat-based measurements presented in this paper did not include CO and CH₄ and therefore only CO₂ was used to calculate EFs from these data. The CRDS data show that CO and CH₄ comprised ~5% and ~10% of the measured C (sum of CO₂, CO and CH₄) for the grass burns and forest fire. These results and consideration of previous studies (Urbanski 2014; Yokelson *et al.* 2013) indicate that using only CO₂ in the C balance calculations would inflate EFs by less than 15%, a value within the total error of the method and likely the reproducibility of the event.

Modified combustion efficiency (MCE), a measure of the fire behaviour's phase, was calculated as:

$$\frac{\Delta CO_2}{\Delta CO + \Delta CO_2} \quad (2)$$

using the CO and CO₂ concentrations collected by the SUMMA canisters and continuous measurements in the airplane.

For the DustTraks, custom correction factors were calculated according to the manufacturer's recommendations (TSI 2010) for DustTraks 8520 and DRX by dividing the average continuous PM_{2.5} concentration by the PM_{2.5} batch filter concentration collected during the same period. The correction factors for DustTrak DRX for grass and forest field burns were 1.6 and 2.4. The DustTrak 8520 had correction factors of 1.9 and 0.91 for forest and grass burns. The EBC and UVPM data from the AE51 and AE52 were post-processed for noise using the optimised noise-reduction averaging algorithm program (Hagler *et al.* 2011).

The single-scattering albedo (SSA) was calculated for each of the three wavelengths (λ) measured by the PASS-3:

$$SSA = \frac{\beta_{scat}}{\beta_{scat} + \beta_{abs}} \quad (3)$$

where β_{scat} is the scattering coefficient and β_{abs} is the absorption coefficient. Low values of SSA indicate that the BC fraction dominates the PM, resulting in positive climate forcing. The absorption angstrom exponent (AAE) describes the spectral variation of the absorption:

$$AAE_{1-2} = \frac{\ln(\beta_{abs}(\lambda_1))/(\beta_{abs}(\lambda_2))}{\ln(\lambda_1)/\ln(\lambda_2)} \quad (4)$$

where $\beta_{abs}(\lambda_1)$ is the absorption coefficient at wavelength 1 (λ_1), and $\beta_{abs}(\lambda_2)$ is the absorption coefficient at wavelength 2 (λ_2). An AAE value near 1 is indicative of urban pollution (i.e. diesel soot), whereas values >1 are associated with brown carbon from biomass burning (Clarke *et al.* 2007). The mass-specific absorption coefficient (MAC) was calculated from the absorption at 781 nm averaged over the same collected time for the EC measurement ($B_{abs}(781 \text{ nm})/EC$).

Results

Ground and aerostat measurements

Fire ignition and fuel type dictated the duration and magnitude of smoke effects downwind from the EBAMs. The grass burns resulted in higher 5-min concentrations whereas the forest understorey burn resulted in higher hourly averages of PM_{2.5} concentrations, which lasted for several hours due to smouldering. For the grass burns, which were short in duration, the PM_{2.5} monitors measured elevated concentrations for only 1–2 h. During the L1G burn, three of the nine deployed EBAMs were affected by the smoke plume with 5-min and hourly maximum PM_{2.5} concentration values of ~2300 $\mu\text{g m}^{-3}$ and 500 $\mu\text{g m}^{-3}$, respectively (Fig. 3a). Both maximums occurred 50 m from the burn perimeter. During the L2F burn, PM_{2.5} concentrations were measured for ~10 h at all 11 EBAMs. The box plots of hourly PM_{2.5} concentrations demonstrate the range of PM_{2.5} concentration values measured during the onset and passage of the primary smoke plume and also during the smouldering phase, which extended into the evening (Fig. 3b). The maximum hourly PM_{2.5} concentration value was ~1100 $\mu\text{g m}^{-3}$ and the maximum 5-min PM_{2.5} concentration was ~1500 $\mu\text{g m}^{-3}$ (not shown).

Emission factors for PM_{2.5} (EFPM_{2.5}) from ground and aerostat measurements for L2F (Table 3) were higher (20 and 23 g kg⁻¹) than those derived in a previous study from the same location and sampling team (14 g kg⁻¹, Aurell and Gullett 2013), possibly due to differences in biomass characteristics. A slightly higher emission factor was found for L2F compared with L2G. Aerostat and ground PM_{2.5} concentrations were similar, with the ground measurements ~10% higher. Particle size results showed that ≥98% of the particulate matter from both burns comprised PM₁ (particles ≤1 μm in aerodynamic diameter) (Fig. 4). The particle distribution for L2F showed a

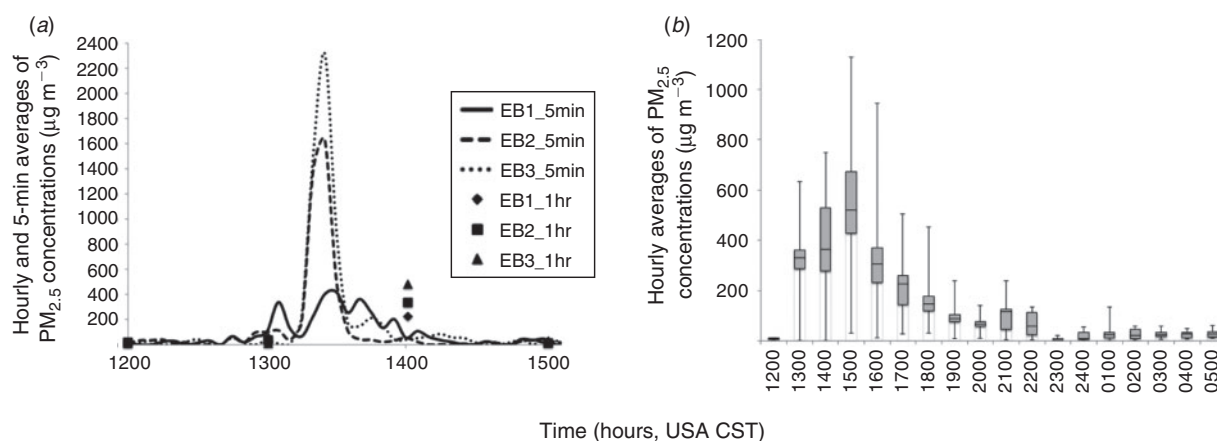


Fig. 3. (a) Ground-based 5-min and hourly $PM_{2.5}$ concentration averages as measured by three of the nine Environmental Beta Attenuation Monitors (EBAMs) deployed that were affected by smoke during L1G (grass burn). EB1, 2 and 3 were located on the north-east side of the burn, with EB1 the furthest east (or furthest right as viewed in Fig. 1a, where EB4 is the corner). Ignition of the burn started at 1230 hours CST and ended at 1346 hours CST. (b) Box plot of ground-based hourly $PM_{2.5}$ concentration averages as measured by the EBAMs deployed during the L2F (forest understorey) burn. The prescribed burn ignition started at 1202 hours CST and ended at 1500 hours CST. Median values are shown as the centre line across the box with the first and third quartile values as the lower and upper lines of the box, respectively. Whiskers extend to the minimum and maximum values.

Table 3. $PM_{2.5}$, equivalent black carbon (EBC), particular matter absorption in the ultraviolet (UVPM), elemental carbon (EC) and organic carbon (OC) emission factors and PM single-scattering albedo (SSA), absorption angstrom exponent (AAE), and mass-specific absorption coefficient (MAC)

Compound	Units	Grass burn (L2G)		Forest burn (L2F)	
		Ground	Aerostat	Ground	Aerostat
Filter $PM_{2.5}$	$g\ kg^{-1}$	18	14	23 ± 1.8^C	20
Continuous $PM_{2.5}$	$g\ kg^{-1}$	20	15	25	24
Continuous EBC ^A	$g\ kg^{-1}$	1.1	0.91	0.89	1.4
Continuous UVPM	$g\ kg^{-1}$	1.8	NS	NS	0.92
Filter EC	$g\ kg^{-1}$	0.62	0.56	0.39 ± 0.16^C	0.46
Filter OC	$g\ kg^{-1}$	7.0	6.5	15 ± 1.8^C	11.3
EBC/ $PM_{2.5}^B$	mass ratio (%)	6.8	7.0	3.6 ± 0.67^C	7.0
EC/ $PM_{2.5}$	mass ratio (%)	3.5	3.9	1.6 ± 0.54^C	2.3
SSA 405 nm		0.78		0.83	
SSA 532 nm		0.83		0.87	
SSA 781 nm		0.76		0.87	
AAE (405–532 nm)		2.60		2.81	
AAE (532–781 nm)		2.09		1.63	
MAC 781 nm	$m^2\ g^{-1}$	5.78		8.02 ± 1.56	

^ANot simultaneously sampled with batch filter.

^BBatch filter and EBC simultaneously sampled.

^COne standard deviation.

higher percentage of PM_1 compared with L2G. Data were collected from a higher altitude during L2F (50–110 m AGL) than during L2G (2 m AGL), suggesting that both biomass type and particle settling effects may have been responsible for these size differences. The latter theory supports the slightly higher EFs measured on the ground vs those from the air on the aerostat platform (Table 3).

EBC (light-absorbing aerosol in the infrared spectrum) and UVPM (light-absorbing organic matter aerosols found in the ultraviolet spectrum) emission factors (EF_{EBC}, EF_{UVPM})

from L2F were 0.89–1.4 $g\ kg^{-1}$ and 0.92–1.8 $g\ kg^{-1}$, respectively (Fig. 5). The EF_{EBC}s are similar to those previously reported from forest understorey burns (1.4 and 2.7 $g\ kg^{-1}$) in the same area and sampling team using the same methods (Aurell and Gullett 2013). No differences in EF_{EBC} between forest and grass burns were detected. The EBC EFs were ~50% lower than the simultaneously sampled EC EFs (Fig. 5). This is in agreement with a previous study by Yelverton *et al.* (2014) that found the EBC concentration to be 39% lower than EC using the same measuring techniques as used in this study.

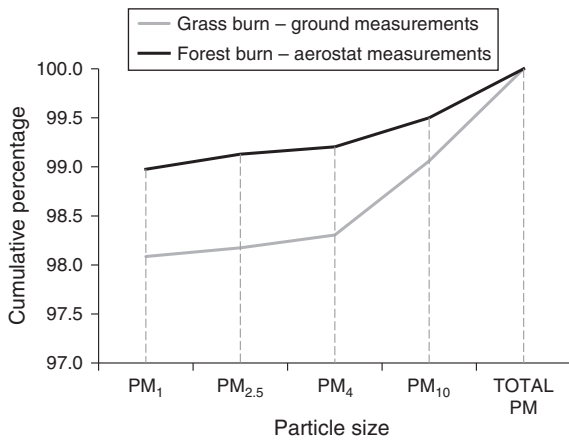


Fig. 4. Particle size distributions from continuous measurements during the L2G and L2F burns.

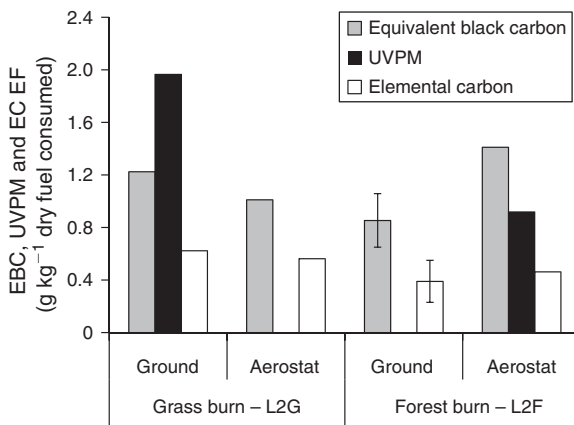


Fig. 5. Equivalent black carbon (EBC), particulate matter absorption in the ultraviolet (UVPM) and elemental carbon (EC) emission factors derived from the L2G (grass) and L2F (forest understorey) burns from mixing ratios sampled near the ground and aloft.

MCE values were compared with simultaneously sampled EFEB (Fig. 6). The ground-sampled EFEB derived from L2F agreed with previously reported data from forest understorey burns (Aurell and Gullett 2013), showing higher EFEB with increased MCE. The aerostat-lofted EFEB (2.4 g kg^{-1}) was higher than that from the ground (1.4 g kg^{-1}) for the same MCE, perhaps indicating a bias of EBC towards smaller particles, which were found to be in greater proportions aloft. Derived EFEB from L2G were lower than those derived from L2F for the same range of MCE.

There were subtle differences in the characteristics of particles emitted from L2G, compared with L2F. L2G emissions exhibited a higher EC : $\text{PM}_{2.5}$ ratio and lower SSA values compared with L2F (Table 3). Emissions from L2F had a slightly larger AAE, indicating a larger brown carbon contribution compared with L2G. The L2F MAC was also elevated, which suggests an internally mixed aerosol where the organic C has condensed onto the surface of elemental C particles and amplified their

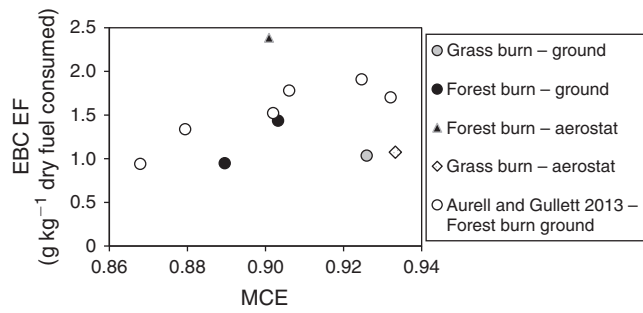


Fig. 6. Equivalent black carbon (EBC) emission factors with respect to measured modified combustion efficiency (MCE). Data from Aurell and Gullett (2013) are also shown; these data were derived in an earlier study near the location of this study. The label ‘Forest burn’ in the figure indicates forest understorey burn, similar to L2F of this study.

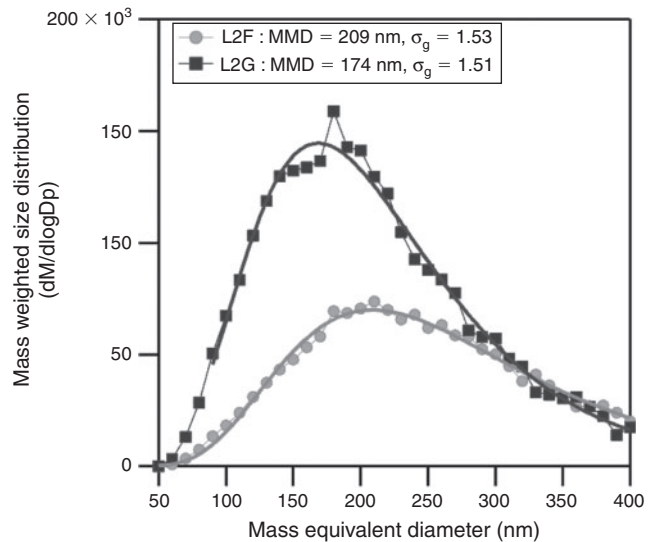


Fig. 7. Representative refractory black carbon (rBC) size distribution measured by the SP2 during the L2G (grass) and L2F (forest understorey) fires. Data are fit with a log-normal distribution (solid lines) to determine the mass median diameter (MMD).

absorption (Lack and Cappa 2010). The rBC size distribution also differed between the L2F and L2G (Fig. 7). The rBC mass median diameter (MMD) from L2F was 20% larger than that measured during L2G. Overall, the particle characteristics suggest that L2F had a larger smouldering contribution compared with L2G.

The EBC fraction and the PM optical properties varied over the duration of the L2F fire (Fig. 8). Early in the fire there was a large spike in the EBC : $\text{PM}_{2.5}$ ratio, which corresponded with the lowest observed SSA of 0.58. As the burn progressed, the EBC : $\text{PM}_{2.5}$ ratio slowly decreased as SSA slowly increased. This trend corresponds with the decrease in MCE that was measured with the aircraft and further demonstrates the relationship between BC emissions and the phase of the fire, with more BC emitted during the flaming phase.

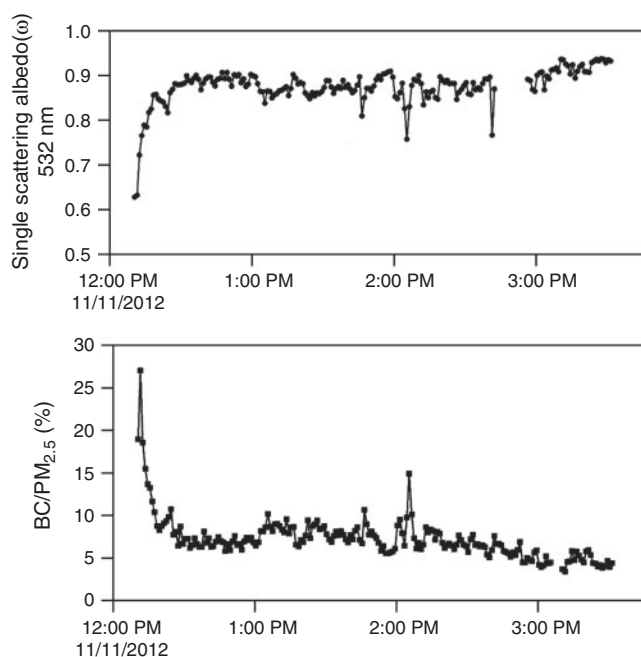


Fig. 8. One-min averaged single-scattering albedo (SSA) and EBC/PM_{2.5} ratio for the L2F (forest understorey) fire.

Aircraft measurements

All three fires (L1G, L2G and L2F) were sampled from ignition until smoke produced by the smouldering fire was no longer lofted high enough to be sampled by the aircraft (~160 m AGL). The sampling period covered 90 min (L1G) to 150 min (L2F) during which 10–30 smoke samples were collected for each fire. The smoke emission samples were obtained between 700 m and 14 000 m downwind from the burn units at altitudes of 160–1530 m above mean sea level. Mixing ratios found in a smoke sample from the L2F fire are shown in Fig. 9. Table S1 in the Supplementary material (available online only) gives the emission factors, MCE, ΔX , altitude and estimated time of emission (ETE) for each smoke sample. The horizontal distance covered by each sample and the number of data points varied with the flight profile, aircraft speed, source strength and dispersion conditions. The typical aircraft groundspeed during smoke sampling was 64 m s⁻¹. The ETE were derived from the wind speed at the altitude of the sample and the average distance of the sample leg from the centroid of the burn unit. The wind speed data from the post-fire atmospheric soundings (Clements *et al.* 2015) were used in the ETE calculations.

The fire-averaged MCE and emission factors for the grass-dominated units (L1G and L2G) were in close agreement with differences of <1% for MCE and EFCO₂, and ~3% and 11% for EFCO and EFCH₄, respectively (Table 4). Although the averages were similar, the variance of MCE and the emissions factors for L1G were twice that of L2G, indicating a wider range of fire behaviour in which the samples were taken. The forested unit burned with a significantly lower MCE and had EFCO and EFCH₄ that were 2 and 2.6 times the grass unit averages, respectively (Table 4).

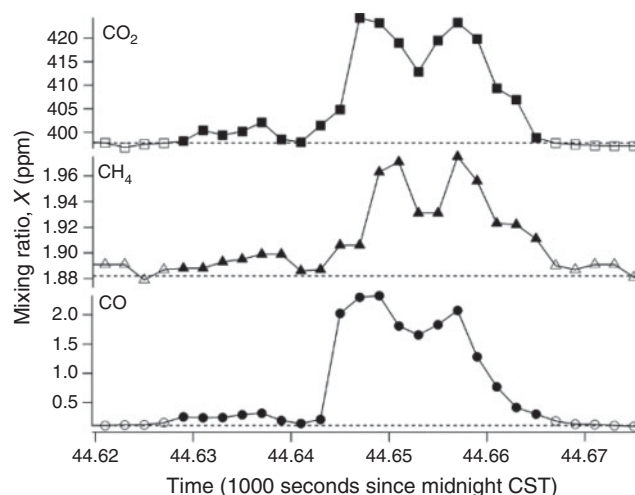


Fig. 9. Cavity ring-down spectroscopy (CRDS) aircraft-based measurements of CO₂, CH₄ and CO mixing ratios for smoke sample run L2F03 of the L2F (forest understorey) fire. The solid markers denote the data points used as the smoke sample. The horizontal dashed line in each panel shows the background mixing ratios measured in the smoke-free air before plume penetration. The markers are 0.5 Hz data points plotted vs time given as 1000 s since midnight (ssm) CST (e.g. 44 640 ssm is 1224 hours CST).

During the L2F fire, EFCH₄ and to a lesser extent MCE varied with ETE (Fig. 10), with EFCH₄ increasing over the course of the fire and MCE decreasing. This behaviour is consistent with a greater contribution from smouldering combustion during the later stages of the fire. However, the different temporal patterns in MCE and EFCH₄ (not shown) suggest they relate differently to fuel components and the combustion process. There was no correlation of EFCH₄ (or MCE) with altitude or distance from the source, indicating that the trend was not an artefact of the smoke sampling pattern nor length of time the smoke was in the atmosphere before sampling. For the L2F fire a linear least square regression of EFCH₄ vs MCE yielded the following fit: $y = 54.4 - 55.3x$ ($R^2 = 0.42$). There was no significant correlation between EFCH₄ and MCE for either the L1G or the L2G fire.

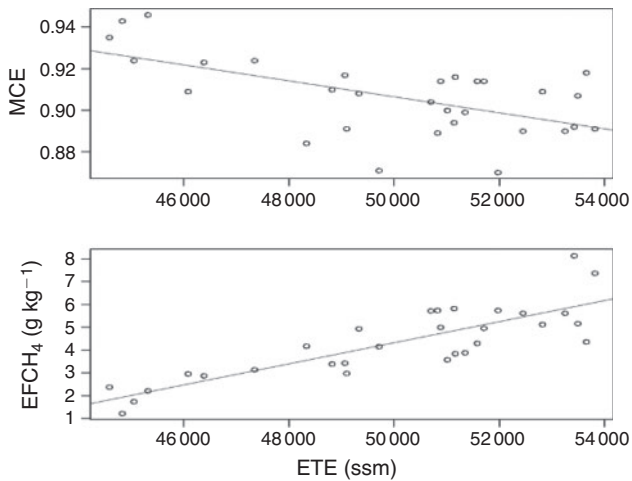
Discussion

PM_{2.5} ground concentrations

Concentrations of PM_{2.5} during both grass burns differed little with elevated concentrations over a short duration but with peaks greater than the forest understorey burn. The forest understorey burn produced elevated concentrations that lasted well after the cessation of ignition due to smouldering fuels. Maximum hourly PM_{2.5} concentrations were higher than that found during the grass burns; however, maximum 5-min PM_{2.5} concentrations were lower than the grass burns. This combination demonstrates the slower pace of the L2F burn compared with the L1G and L2G burns, as well as the quantity of L2F smouldering fuels. Differences between the aerostat and ground PM_{2.5} concentrations measured during L2G and L2F were small with slightly higher concentrations measured near the ground. Data from these burns suggest that larger particles may settle out with altitude, placing larger particles closer to the ground.

Table 4. Aircraft-based measurements of fire-averaged modified combustion efficiency (MCE) and emission factors (EF) (± 1 standard deviation)

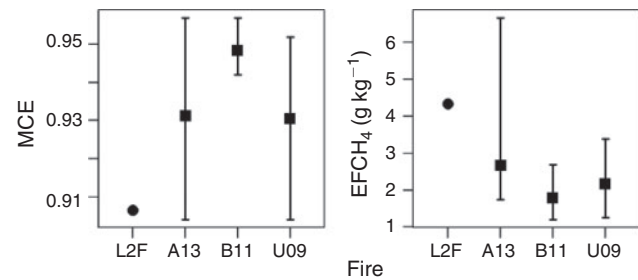
	Number of samples	MCE	EF _{CO₂} (g kg ⁻¹)	EF _{CO} (g kg ⁻¹)	EF _{CH₄} (g kg ⁻¹)
L1G	30 ^A	0.950 \pm 0.016	1738 \pm 29	58.4 \pm 18.9	1.75 \pm 0.96
L2G	10 ^B	0.953 \pm 0.005	1743 \pm 8	55.0 \pm 5.4	1.57 \pm 0.48
L2F	30	0.906 \pm 0.019	1651 \pm 37	108.4 \pm 21.4	4.32 \pm 1.58

^AEF_{CH₄} is based on 21 samples.^BEF_{CH₄} is based on 7 samples.**Fig. 10.** Cavity ring-down spectroscopy (CRDS) aircraft measured modified combustion efficiency (MCE) (top) and methane emission factor (EF_{CH₄}) (bottom) plotted vs the estimated time of emission (ETE, see text) for the L2F (forest understory) fire. ETE is plotted in seconds since midnight (ssm) CST (e.g. 44 640 ssm is 1224 hours CST). Solid lines are linear least-squares fits. The Spearman's rank correlation with ETE was $r = -0.48$ ($P < 0.01$) for MCE and $r = 0.80$ ($P < 0.0001$) for EF_{CH₄}.

Emission factors

The fuels consumed in the L1G and L2G fires consisted largely of grass and forbs (78% and 76%) with litter and shrubs constituting the balance (Ottmar *et al.* 2015). In contrast, grass and forb consumption was negligible in L2F, where litter (pine and hardwood), dead woody debris and shrubs accounted for 79%, 15%, and 6% of the total fuel consumed (Ottmar *et al.* 2015). The fuel consumption measurements suggest that though grass and litter are both classified as fine fuels (fuel particles with a high surface to volume ratio), the latter burned with a significantly lower MCE (and produced higher EFCO and EF_{CH₄}). Urbanski (2014) examined MCE and fuel consumption data from 18 prescribed fires and found that when fuel consumption was dominated by fine fuels (litter, grasses, shrubs and fine woody debris) high MCE was favoured. All the fires in this study were dominated by fine fuel consumption but each burned with a different MCE and produced different emission factors. This suggests that the composition and characteristics of fine fuels (grass and forbs vs litter and woody debris) are important factors influencing emissions.

The grass-dominated units burned with high MCE and low EFCO and EF_{CH₄}, in contrast to the forested unit – a finding that is consistent with previous studies. Comparing the L2F results

**Fig. 11.** Fire-averaged modified combustion efficiency (MCE) and EF_{CH₄} for the forest understory, L2F, fire (solid circle) and previous study averages (solid squares) of MCE (left) and methane emission factor (EF_{CH₄}) (right). The previous studies reported fire-averaged emission factors (EF) for multiple fires and the whiskers denote the range of the fire-averaged EF from these studies. A13 = Akagi *et al.* 2013 with seven fires; B11 = Burling *et al.* 2011 with six fires in North Carolina only; U09 = Urbanski *et al.* 2009 with 21 fires.

with previous field studies of emissions from prescribed fires in pine-dominated forests of the southeastern US (Fig. 11), the L2F MCE is at the low end of the fire-averaged values reported by Akagi *et al.* (2013), Burling *et al.* (2011) and Urbanski *et al.* (2009). Six fires included as grasslands and shrublands in Urbanski *et al.* (2009) were actually forest understory burns (EB1, EB2, FL5, SC9, FS1 and ICI3). We have included these six fires in our analysis. In terms of carbon, CH₄ is the dominant organic gas released by prescribed fires and so we compare our EF_{CH₄} values with those reported in these three previous field studies. Of these, the EF_{CH₄} of only one fire exceeds our L2F EF_{CH₄} and that fire's MCE is substantially lower than the average of the 34 fires reported in these three studies (0.906 vs 0.934). Our EF_{CH₄} value (4.32 g kg⁻¹) is close to the value predicted by the EF_{CH₄} vs MCE regression equation (4.44 g kg⁻¹) reported in Akagi *et al.* (2013). Conversely, using all 34 previously published fires the EF_{CH₄} vs MCE linear equation ($y = 47.3 - 48.3x$; $R^2 = 0.47$) predicts an EF_{CH₄} of 3.54 g kg⁻¹ for L2F (with an MCE of 0.906), ~20% below the observed value.

We compared our results from the grass burns (L1G and L2G) with eight grassland burns (EP1, EP2A, EP2B, M11, MN1, MN2, MN3 and MN4) reported in Urbanski *et al.* (2009). L1G and L2G fires have similar MCE and emission factor values to these eight grassland fires, which have an average MCE of 0.945 and corresponding EF_{CH₄} of 1.95 g kg⁻¹. Our values are 10% (L1G) and 19% (L2G) below this grassland fire average. These small differences are attributed to the MCE. A linear least square regression, using the eight grassland fires, of EF_{CH₄} vs MCE

yields the following fit: $y = 54.0 - 55.0x$ ($R^2 = 0.92$). This equation predicts EFCH₄ of 1.75 g kg⁻¹ for L1G and 1.59 g kg⁻¹ for L2G. This agrees with those measured in our study.

Particulate characteristics

There are a limited number of *in situ* measurements of fresh biomass plume optical properties and to our knowledge none for the southeastern US. Our SSAs for L2G and L2F fall within the range of 0.8–0.9 (at 540 nm) reported for wildfires and prescribed burns in the western US and Canada (Radke *et al.* 1988, 1991). A lower SSA for the grass-dominated unit compared with the forested unit was also observed by Reid and Hobbs (1998), who measured an SSA of 0.76 for grass and of 0.84 for smouldering slash and standing forest fires in Brazil. SSA values from different fuels in the laboratory measurements have been mixed, with no consistent difference between grasses and trees (litter and woody debris) or shrubs (Lewis *et al.* 2008; Mack *et al.* 2010).

The AAE measured during the L2G and L2F burns were somewhat higher than other measurements in fresh plumes and indicate that there may have been more brown carbon or brown carbon with varying optical properties. For example, Corr *et al.* (2012) measured 1.38 (470–573 nm) in a fresh boreal plume compared with the 2.44 and 3.01 (405–532 nm) we observed for the L2G and L2F burns, respectively. Laboratory measurements by Lewis *et al.* (2008) found a large range of AAE of 0.86–3.48 (405–870 nm), which depended on the fuel. However, it is difficult to compare AAE across studies as different measurement methods can provide very different results (Corr *et al.* 2012), and these results are dependent upon the wavelength range investigated, as biomass burning PM exhibits increasing AAE with decreasing wavelength (Lewis *et al.* 2008; Sandradewi *et al.* 2008; Corr *et al.* 2012).

The rBC MMD of 209 nm measured for the forested unit is similar to the average 193 nm found in fresh prescribed and wildfire plumes in California (Sahu *et al.* 2012), 187 nm for fresh boreal wildfire plumes (Kondo *et al.* 2011) and 210 nm for plumes (likely brush fires) over Texas (Schwarz *et al.* 2008). We have assumed an rBC density of 1.8 g cm⁻³ for our calculations, which makes our MMD ~3% larger than that previously measured, where the assumed density was 2 g cm⁻³. The difference in sizes between the fires at L2G and L2F (Fig. 7) are approximately within the variation observed by Kondo *et al.* (2011) in fresh and aged smoke plumes produced by boreal forest fires. Although Kondo *et al.* (2011) observed a slight trend of decreasing rBC size with increasing MCE, they could not account for the influence of different vegetation.

Conclusion

Comparing the time evolution of PM_{2.5} concentration data between the grass and forest understory burns highlights the importance of understanding how the hourly concentration is derived, either from consistent elevated concentrations (L2F) or from acute peaks that are short in duration (L1G). This has implications for firefighter health and safety in that high concentrations for short durations may be a concern for fitness and visibility. In addition, the forest understory burned with

a different MCE and produced different emission factors compared with other studies done in this region. The particle characteristics of SSAs and EC : PM_{2.5} ratio suggest that L2F had a larger smouldering contribution than did L2G. This indicates that the composition and characteristic mosaic of the fine fuels (grass and forbs vs litter and woody debris) are important factors influencing emissions. Models deriving smoke emissions and predicting smoke concentrations may need to take into account the full fuel mosaic rather than just general fuel conditions. Numerous smoke measurements were made during the RxCADRE 2012 field campaign, and the results show the value of combining multiple smoke measurements at multiple heights to enhance our understanding of the evolution of smoke concentrations and emissions during a controlled burn.

Acknowledgements

This work was funded by the Joint Fire Science Program (Project #11-2-1-11), the Strategic Environmental Research and Development Program (Dr John Hall) and the US EPA Office of Research and Development. This research was performed while Johanna Aurell held a National Research Council Research Associateship Award at the US EPA/NRMRL. We would like to thank Dave Hubble, our mission Cessna 337 pilot, and Aaron Knobloch of USFS Southern Region for his support in facilitating the airplane arrangements. Contributing EPA personnel included Chris Pressley, Bill Squier, Bill Mitchell, Michael Hays and Robert Black (Oak Ridge Institute for Science and Education postdoctoral fellow). Aerostat operations were handled by Rob Gribble (ISSI Inc.). Jeff Blair of AethLabs donated use of the AE-52. We also thank Candace Krull for her assistance with preparing field equipment before the study and Gary Curcio for contributing instrumentation, expertise and aid in deploying the equipment. We also give a special thanks to Scott Pokswinski (aka Daisycutter) who watched out for us while at the field site. The use of trade or firm names in this publication is for reader information and does not imply endorsement by the US Department of Agriculture and Environmental Protection Agency of any product or service.

References

- Akagi SK, Yokelson RJ, Wiedinmyer C, Alvarado MJ, Reid JS, Karl T, Crounse JD, Wennburg PO (2010) Emission factors for open and domestic biomass burning for use in atmospheric models. *Atmospheric Chemistry and Physics Discussion* **10**, 27 523–27 602. doi:10.5194/ACPD-10-27523-2010
- Akagi SK, Yokelson RJ, Burling IR, Meinardi S, Simpson I, Blake DR, McMeeking GR, Sullivan A, Lee T, Kreidenweis S, Urbanski S, Reardon J, Griffith DWT, Johnson TJ, Weise DR (2013) Measurements of reactive trace gases and variable O₃ formation rates in some South Carolina biomass burning plumes. *Atmospheric Chemistry and Physics* **13**, 1141–1165. doi:10.5194/ACP-13-1141-2013
- Andreae MO, Merlet P (2001) Emission of trace gases and aerosols from biomass burning. *Global Biogeochemical Cycles* **15**, 955–966. doi:10.1029/2000GB001382
- Aurell J, Gullett BK (2013) Emission factors from aerial and ground measurements of field and laboratory forest burns in the southeastern US: PM_{2.5}, black and brown carbon, VOC, and PCDD/PCDF. *Environmental Science & Technology* **47**, 8443–8452. doi:10.1021/ES402101K
- Aurell J, Gullet BK, Pressley C, Tabor DG, Gribble RD (2011) Aerostat-lofted instrument and sampling method for determination of emissions from open area sources. *Chemosphere* **85**, 806–811. doi:10.1016/J.CHEMOSPHERE.2011.06.075
- Bond TC, Doherty SJ, Fahey DW, Forster PM, Bernsten T, DeAngelo BJ, Flanner MG, Ghan S, Kärcher B, Koch D, Kinne S, Kondo Y, Quinn PK, Sarofim MC, Schulz M, Venkataraman C, Zhang H, Zhang S,

- Bellouin N, Guttikunda SK, Hopke PK, Jacobson MZ, Kaiser JW, Klimont Z, Lohmann U, Schwarz JP, Shindell D, Storelvmo T, Warren SG, Zender CS (2013) Bounding the role of black carbon in the climate system: a scientific assessment. *Journal of Geophysical Research, D, Atmospheres* **118**, 5380–5552. doi:10.1002/JGRD.50171
- Burling IR, Yokelson RJ, Griffith DWT, Johnson TJ, Veres P, Roberts JM, Warneke C, Urbanski SP, Reardon J, Weise DR, Hao WM, de Gouw J (2010) Laboratory measurements of trace gas emissions from biomass burning of fuel types from the southeastern and southwestern United States. *Atmospheric Chemistry and Physics* **10**, 11115–11130. doi:10.5194/ACP-10-11115-2010
- Burling IR, Yokelson RJ, Akagi SK, Urbanski SP, Wold CE, Griffith DWT, Johnson TJ, Reardon J, Weise DR (2011) Airborne and ground-based measurements of the trace gases and particles emitted by prescribed fires in the United States. *Atmospheric Chemistry and Physics* **11**, 12197–12216. doi:10.5194/ACP-11-12197-2011
- Chung CE, Ramanathan V, Decremier D (2012) Observationally constrained estimates of carbonaceous aerosol radiative forcing. *Proceedings of the National Academy of Sciences of the United States of America* **109**, 11624–11629. doi:10.1073/PNAS.1203707109
- Clarke A, McNaughton C, Kapustin V, Shinozuka Y, Howell S, Dibb J, Zhou J, Anderson B, Brekhovskikh V, Turner H, Pinkerton M (2007) Biomass burning and pollution aerosol over North America: organic components and their influence on spectral optical properties and humidification response. *Journal of Geophysical Research, D, Atmospheres* **112**, D12S18. doi:10.1029/2006JD007777
- Clements CB, Lareau NP, Seto D, Contezac J, Davis B, Teske C, Zajkowski TJ, Hudak AT, Bright BC, Dickinson MB, Butler BW, Jimenez D, Hiers JK (2015) Fire weather conditions and fire–atmosphere interactions observed during low-intensity prescribed fires – RxCADRE 2012. *International Journal of Wildland Fire* **25**, 90–101. doi:10.1071/WF14173
- Corr CA, Hall SR, Ullmann K, Anderson BE, Beyersdorf AJ, Thornhill KL, Cubison MJ, Jimenez JL, Wisthaler A, Dibb JE (2012) Spectral absorption of biomass burning aerosol determined from retrieved single scattering albedo during ARCTAS. *Atmospheric Chemistry and Physics* **12**, 10505–10518. doi:10.5194/ACP-12-10505-2012
- Flowers BA, Dubey MK, Mazzoleni C, Stone EA, Schauer JJ, Kim SW, Yoon SC (2010) Optical–chemical–microphysical relationships and closure studies for mixed carbonaceous aerosols observed at Jeju Island; 3-laser photoacoustic spectrometer, particle sizing, and filter analysis. *Atmospheric Chemistry and Physics* **10**, 10387–10398. doi:10.5194/ACP-10-10387-2010
- French NH, de Groot WJ, Jenkins LK, Rogers BM, Alvarado E, Amiro B, de Jong B, Goetz S, Hoy E, Hyer E, Keane R, Law BE, McKenzie D, McNulty SG, Ottmar R, Pérez-Saliciup DR, Randerson J, Robertson KM, Turetsky M (2011) Model comparisons for estimating carbon emissions from North American wildland fire. *Journal of Geophysical Research: Biogeosciences* **116**, G00K05. doi:10.1029/2010JG001469
- Goode JG, Yokelson RJ, Susott R A, Ward DE (1999) Trace gas emissions from laboratory biomass fires measured by open-path Fourier transform infrared spectroscopy: fires in grass and surface fuels. *Journal of Geophysical Research: Atmospheres* **104**, 21237–21245. doi:10.1029/1999JD900360
- Hagler GSW, Yelverton TLB, Vedantham R, Hansen ADA, Turner JR (2011) Post-processing method to reduce noise while preserving high time resolution in aethalometer real-time black carbon data. *Aerosol and Air Quality Research* **11**, 539–546. doi:10.4209/AAQR.2011.0055
- Hobbs PV, Reid JS, Kotchenruther RA, Ferek RJ, Weiss R (1997) Direct radiative forcing by smoke from biomass burning. *Science* **275**, 1777–1778. doi:10.1126/SCIENCE.275.5307.1777
- Hodzic A, Madronich S, Bohn B, Massie S, Menut L, Wiedinmyer C (2007) Wildfire particulate matter in Europe during summer 2003: mesoscale modeling of smoke emissions, transport and radiative effects. *Atmospheric Chemistry and Physics* **7**, 4043–4064. doi:10.5194/ACP-7-4043-2007
- Khan B, Hays MD, Geron C, Jetter J (2012) Differences in the OC/EC ratios that characterize ambient and source aerosols due to thermal-optical analysis. *Aerosol Science and Technology* **46**, 127–137. doi:10.1080/02786826.2011.609194
- Kondo Y, Matsui H, Moteki N, Sahu L, Takegawa N, Kajino M, Zhao Y, Cubison MJ, Jimenez JL, Vay S, Diskin GS, Anderson B, Wisthaler A, Mikoviny T, Fuelberg HE, Blake DR, Huey G, Weinheimer AJ, Knapp DJ, Brune WH (2011) Emissions of black carbon, organic, and inorganic aerosols from biomass burning in North America and Asia in 2008. *Journal of Geophysical Research, D, Atmospheres* **116**, D08204. doi:10.1029/2010JD015152
- Lack DA, Cappa CD (2010) Impact of brown and clear carbon on light absorption enhancement, single scatter albedo and absorption wavelength dependence of black carbon. *Atmospheric Chemistry and Physics* **10**, 4207–4220. doi:10.5194/ACP-10-4207-2010
- Larkin NK, Raffuse SM, Strand TM (2014) Wildland fire emissions, carbon, and climate: US emissions inventories. *Forest Ecology and Management* **317**, 61–69. doi:10.1016/J.FORECO.2013.09.012
- Laursen KK, Ferek R, Hobbs P, Rasmussen RA (1992) Emission factors for particles, elemental carbon, and trace gases from the Kuwait oil fires. *Journal of Geophysical Research, D, Atmospheres* **97**, 14491–14497. doi:10.1029/92JD01370
- Lewis K, Arnott WP, Moosmüller H, Wold CE (2008) Strong spectral variation of biomass smoke light absorption and single scattering albedo observed with a novel dual-wavelength photoacoustic instrument. *Journal of Geophysical Research, D, Atmospheres* **113**, D16203. doi:10.1029/2007JD009699
- Li G, Bei N, Tie X, Molina LT (2011) Aerosol effects on the photochemistry in Mexico City during MCMA-2006/MILAGRO campaign. *Atmospheric Chemistry and Physics* **11**, 5169–5182. doi:10.5194/ACP-11-5169-2011
- Mack LA, Levin EJT, Kreidenweis SM, Obrist D, Moosmüller H, Lewis KA, Arnott WP, McMeeking GR, Sullivan AP, Wold CE, Hao W-M, Collett JL, Malm WC (2010) Optical closure experiments for biomass smoke aerosols. *Atmospheric Chemistry and Physics* **10**, 9017–9026. doi:10.5194/ACP-10-9017-2010
- McMeeking GR, Kreidenweis SM, Lunden M, Carrillo J, Carrico CM, Lee T, Herckes P, Engling G, Day DE, Hand J, Brown N, Malm WC, Collett JL, Jr (2006) Smoke-impacted regional haze in California during the summer of 2002. *Agricultural and Forest Meteorology* **137**, 25–42. doi:10.1016/J.AGRFORMET.2006.01.011
- National Institute for Occupation Safety and Health (NIOSH) (1999) Method 5040: elemental carbon (diesel particulate). Available at <http://www.cdc.gov/niosh/docs/2003-154/pdfs/5040.pdf> [Verified 12 October 2015]
- Ottmar RD, Hudak AT, Prichard SJ, Wright CS, Restaino JC, Kennedy MC, Vihnanek RE (2015) Pre-fire and post-fire surface fuel and cover measurements collected in the southeastern United States for model evaluation and development – RxCADRE 2008, 2011 and 2012. *International Journal of Wildland Fire* **25**, 10–24. doi:10.1071/WF15092
- Petzold A, Ogren JA, Fiebig M, Laj P, Li S-M, Baltensperger U, Holzner-Popp T, Kinne S, Pappalardo G, Sugimoto N, Wehrli C, Wiedensohler A, Zhang X-Y (2013) Recommendations for reporting ‘black carbon’ measurements. *Atmospheric Chemistry and Physics* **13**, 8365–8379. doi:10.5194/ACP-13-8365-2013
- Radke LF, Hegg DA, Lyons JH, Brock CA, Hobbs PV, Weiss RE, Rasmussen R (1988) Airborne measurements on smokes from biomass burning. In ‘Aerosols and Climate’. (Eds PV Hobbs, MP McCormick), pp. 411–422. (Deepak Publishing: Hampton, VA)
- Radke LF, Hegg DA, Hobbs PV, Nance JD, Lyons JH, Larsen KK, Weiss RE, Regan PJ, Ward DE (1991) Particulate and trace emissions from large biomass fires in North America. In ‘Global Biomass

- Burning: Atmospheric, Climate, and Biospheric Implications.' (Ed. JS Levine) pp. 209–224. (MIT Press: Cambridge, MA)
- Reid JS, Hobbs PV (1998) Physical and optical properties of young smoke from individual biomass fires in Brazil. *Journal of Geophysical Research, D, Atmospheres* **103**, 32 013–32 030. doi:10.1029/98JD00159
- Sahu LK, Kondo Y, Moteki N, Takegawa N, Zhao Y, Cubison MJ, Jimenez JL, Vay S, Diskin GS, Wisthaler A, Mikoviny T, Huey LG, Weinheimer AJ, Knapp DJ (2012) Emission characteristics of black carbon in anthropogenic and biomass burning plumes over California during ARCTAS–CARB 2008. *Journal of Geophysical Research, D, Atmospheres* **117**, D16302. doi:10.1029/2011JD017401
- Sandradewi J, Prevot ASH, Weingartner E, Schmidhauser R, Gysel M, Baltensperger U (2008) A study of wood burning and traffic aerosols in an alpine valley using a multi-wavelength aethalometer. *Atmospheric Environment* **42**, 101–112. doi:10.1016/j.atmosenv.2007.09.034
- Schwarz JP, Gao RS, Fahey DW, Thomson DS, Watts LA, Wilson JC, Reeves JM, Darbeheshti M, Baumgardner DG, Kok GL, Chung SH, Schulz M, Hendricks J, Lauer A, Karcher B, Slowik JG, Rosenlof KH, Thompson TL, Langford AO, Loewenstein M, Aikin KC (2006) Single-particle measurements of midlatitude black carbon and light-scattering aerosols from the boundary layer to the lower stratosphere. *Journal of Geophysical Research, D, Atmospheres* **111**, D16207. doi:10.1029/2006JD007076
- Schwarz JP, Gao RS, Spackman JR, Watts LA, Thomson DS, Fahey DW, Ryerson TB, Peischl J, Holloway JS, Trainer M, Frost GJ, Baynard T, Lack DA, de Gouw JA, Warneke C, Del Negro LA (2008) Measurement of the mixing state, mass, and optical size of individual black carbon particles in urban and biomass burning emissions. *Geophysical Research Letters* **35**, L13810. doi:10.1029/2008GL033968
- Strand T, Larkin N, Rorig M, Krull C, Moore M (2011) PM_{2.5} measurements in wildfire smoke plumes from fire seasons 2005–2008 in the northwestern United States. *Journal of Aerosol Science* **42**, 143–155. doi:10.1016/j.jaerosci.2010.09.001
- TSI (2010) Model 8520 DustTrack aerosol monitor operation and service manual, 1980198 rev. 8, June 2010. Available at http://www.tsi.com/uploadedfiles/_site_root/products/literature/manuals/1980198S-8520.pdf [Verified 14 March 2014]
- Urbanski SP (2013) Combustion efficiency and emission factors for wildfire-season fires in mixed conifer forests of the northern Rocky Mountains, US. *Atmospheric Chemistry and Physics* **13**, 7241–7262. doi:10.5194/ACP-13-7241-2013
- Urbanski SP (2014) Wildland fire emissions, carbon, and climate: emission factors. *Forest Ecology and Management* **317**, 51–60.
- Urbanski SP, Baker SP, Hao WM (2009) Chemical composition of wildland fire emissions. In 'Wildland Fires and Air Pollution'. (Eds A Bytnerowicz, M Arbaugh, A Riebau, C Anderson), pp. 79–107. (Elsevier: Amsterdam, Netherlands)
- Wegesser TC, Pinkerton KE, Last JA (2009) California wildfires of 2008: coarse and fine particulate matter toxicity. *Environmental Health Perspectives* **117**, 893–897. doi:10.1289/EHP.0800166
- Yelverton TLB, Hays MD, Gullett BK, Linak WP (2014) Black carbon measurements of flame-generated soot as determined by optical, thermal-optical, direct absorption, and laser incandescence methods. *Environmental Engineering Science* **31**(4), 209–215. doi:10.1089/EES.2014.0038
- Yokelson R, Goode J, Ward D, Susott R, Babbit R, Wade D, Bertschi I, Griffith D, Hao W (1999) Emissions of formaldehyde, acetic acid, methanol, and other trace gases from biomass fires in North Carolina measured by airborne Fourier transform infrared spectroscopy. *Journal of Geophysical Research, D, Atmospheres* **104**, 30 109–30 125. doi:10.1029/1999JD900817
- Yokelson RJ, Burling IR, Gilman JB, Warneke C, Stockwell CE, de Gouw J, Akagi SK, Urbanski SP, Veres P, Roberts JM, Kuster WC, Reardon J, Griffith DWT, Johnson TJ, Hosseini S, Miller JW, Cocker DR, III, Jung H, Weise DR (2013) Coupling field and laboratory measurements to estimate the emission factors of identified and unidentified trace gases for prescribed fires. *Atmospheric Chemistry and Physics* **13**, 89–116. doi:10.5194/ACP-13-89-2013